Cognitive Light Cones and Resource-Bounded Intelligence

A Geometric Theory of Detect-and-Reach Capacity

Working Draft
November 2024

Abstract

We develop a rigorous mathematical theory connecting an agent's resource constraints to the spatiotemporal scope of goals it can achieve. The central object is the *cognitive light cone*—the region of spacetime an agent can sense or influence—which we formalize as the union of observability and reachability sets within a POMDP framework.

We prove tight bounds on goal achievement capacity as explicit functions of sensing range r, actuation range a, speed v, and time horizon T. In one dimension, we establish that capturable set size is bounded by a piecewise-linear function exhibiting three regimes: detection-limited ($a \geq r$), coupled ($a < r \leq vT + a$), and reach-limited ($r > vT + a$). Each regime has a distinct optimal strategy: monotonic sweeps in the detection-limited and coupled regimes, and a detect-then-pursue policy in the reach-limited regime. We extend these results to two dimensions, deriving stadium-geometry bounds and proving that straight-line trajectories are optimal via a Steiner-type curvature penalty argument.

Finally, we apply these results to a corridor coverage design problem, demonstrating how the theory can be inverted to derive hardware procurement requirements (e.g., minimum robot count and speed) from coverage guarantees.

Contents

1 Introduction

1.1 Motivation

Intelligence, as it exists in the natural world, operates under severe resource constraints. Every biological agent—from single cells to human societies—must achieve goals using limited energy, bandwidth, memory, and time. Yet formal theories of intelligence often abstract away these constraints, treating the agent as having unlimited computational resources.

This paper develops a geometric theory of resource-bounded intelligence. Our central question is:

> *Given an agent with sensing range r, actuation range a, speed v, and time horizon T, what is the maximum spatial extent of goals it can achieve?*

We answer this question precisely for a class of "detect-and-reach" problems, proving tight bounds that exhibit qualitatively distinct regimes depending on how sensing and actuation capabilities relate.

1.2 The Cognitive Light Cone

Our framework is inspired by Michael Levin's concept of the *cognitive light cone* [Levin, 2019, 2025]—the spatiotemporal volume an agent can sense, model, and influence. Levin introduced this concept in the context of developmental biology to describe how cells and organisms exhibit goal-directed behavior at multiple scales.

We formalize the cognitive light cone within the language of Partially Observable Markov Decision Processes (POMDPs). For an agent at position x with sensing range r and actuation range a:

- The **observability cone** $\mathcal{O}(x, r)$ consists of spacetime points whose state can influence the agent's observations.
- The **reachability cone** $\mathcal{R}(x, a, T)$ consists of spacetime points the agent can causally influence.
- The **cognitive light cone** is their union: $L_T = \mathcal{O} \cup \mathcal{R}$.

The light cone defines the boundary of what the agent can "care about"—it cannot pursue goals concerning regions outside this cone.

1.3 Main Contributions

1. **Formal framework:** We ground the cognitive light cone concept in standard POMDP theory, providing precise definitions that connect to control-theoretic notions of observability and controllability.
2. **1D Detect-and-Reach Theorem:** We prove that for a one-dimensional domain, the capturable set size is bounded by:

$$|C(\pi)| \leq \begin{cases} vT + 2r + 1 & a \geq r \\ vT + r + a + 1 & a < r \leq vT + a \\ 2(vT + a) + 1 & r > vT + a \end{cases}$$

   with regime-dependent optimal strategies.

3. **2D Stadium Theorem:** We extend to two dimensions, proving area bounds with stadium geometry and establishing that straight-line trajectories are optimal via a curvature penalty argument.

4. **Regime classification:** We identify three qualitatively distinct regimes—detection-limited, coupled, and reach-limited—with sharp transitions and distinct optimal strategies.

5. **Engineering Application:** We demonstrate the practical utility of the theory by applying it to a multi-robot coverage problem, deriving a "procurement chart" that maps coverage goals to hardware specifications.

1.4 Related Work

Our results connect several literatures:

Data-rate theorems in networked control establish minimum channel capacity for stabilizing dynamical systems [Nair et al., 2007]. We extend this to spatial goal-achievement rather than stabilization.

Finite-memory POMDP approximation provides bounds on how memory constraints limit achievable value [Kara et al., 2021]. We complement this by analyzing spatial rather than memory constraints.

Regional controllability of cellular automata [El Yacoubi et al., 2002] asks whether spatial regions can be controlled, but does not provide quantitative bounds on achievable region size.

Dec-POMDPs with bounded communication [Wu et al., 2011] analyze multi-agent coordination, which our framework can extend to via collective light cones.

To our knowledge, no prior work provides explicit bounds of the form "goal region size $\leq f(r, a, v, T)$" for spatial POMDPs.

1.5 Paper Outline

Section 2 establishes the formal POMDP framework and defines the cognitive light cone precisely. Section 3 develops the 1D theory, stating and proving the Detect-and-Reach Theorem. Section 4 extends to 2D, deriving the stadium bounds and proving straight-line optimality. Section 5 discusses empirical validation. Section 6 presents the multi-agent composition results. Section 7 provides a concrete design example. Section 8 connects our results to biological theory.

2 Theoretical Framework

2.1 POMDP Foundations

We work within the standard POMDP framework [Kaelbling et al., 1998].

Definition 2.1 (POMDP)**.** A *Partially Observable Markov Decision Process* is a tuple $M = (S, A, O, T, Z, R, \gamma, b_0)$ where:

- S is the state space
- A is the action space
- O is the observation space
- $T : S \times A \times S \to [0, 1]$ is the transition function
- $Z : S \times A \times O \to [0, 1]$ is the observation function
- $R : S \times A \to \mathbb{R}$ is the reward function

- $\gamma \in [0, 1)$ is the discount factor
- $b_0 \in \Delta(S)$ is the initial belief state

A *policy* π maps histories to actions. The *value* of policy π from belief b is:

$$V^\pi(b) = \mathbb{E}\left[\sum_{t=0}^{\infty} \gamma^t R(s_t, a_t) \mid b_0 = b, \pi\right]$$

2.2 Time and Space Conventions

Throughout this paper, we adopt the following conventions:

- **Space** is continuous: positions lie in $\mathbb{R}$ (1D) or $\mathbb{R}^2$ (2D).
- **Distances** r, a, and v are real-valued parameters.
- **1D analysis (Section 3):** Time is discrete, $t \in \{0, 1, \ldots, T\}$, with speed constraint $|x_{t+1} - x_t| \leq v$ per unit time step.
- **2D analysis (Section 4):** We work with continuous time $t \in [0, T]$ and trajectories γ satisfying $\|\dot{\gamma}(t)\| \leq v$. This continuous-time formulation only tightens the bounds (fewer admissible paths) and thus the capacity bounds also apply to the discrete-time case.

This mixed formulation is standard in robotics and planning; the discrete-time 1D analysis is simpler to present, while the continuous-time 2D analysis connects directly to classical tube formulas.

2.3 Spatial POMDPs

We consider POMDPs with spatial structure.

Definition 2.2 (Spatial POMDP)**.** A *spatial POMDP* has state space $S = X \times \Theta$, where X is a spatial domain and Θ parameterizes hidden target locations. The agent occupies position $x_t \in X$ and takes actions a_t that determine movement: $|x_{t+1} - x_t| \leq v$ for speed bound v.

Definition 2.3 (Sensing and Actuation Ranges)**.** An agent has:

- *Sensing range* r: At time t, the agent observes all targets within distance r of position x_t.
- *Actuation range* a: The agent can "capture" (affect) targets within distance a of its position.

2.4 The Cognitive Light Cone

Definition 2.4 (Observability Set)**.** For an agent at position x with sensing range r:

$$\mathcal{O}(x, r) = \{y \in X : d(x, y) \leq r\}$$

Definition 2.5 (Reachability Set)**.** For an agent at position x with speed v, actuation range a, at horizon T:

$$\mathcal{R}(x, a, T) = \{y \in X : d(x, y) \leq vT + a\}$$

This is the set of points the agent can reach and act upon by time T.

Definition 2.6 (Cognitive Light Cone)**.** The *cognitive light cone* at time t with horizon T is:

$$L_t(T) = \{(y, \tau) : y \in \mathcal{O}(x_t, r) \text{ for } \tau \leq t, \text{ or } y \in \mathcal{R}(x_t, a, T - t) \text{ for } \tau > t\}$$

This is the set of spacetime points the agent can have known about (past) or can influence (future).

2.5 The Intelligence Functional

Following Legg and Hutter [2007], we define intelligence as goal-achievement across environments.

Definition 2.7 (Resource-Bounded Intelligence)**.** Let $\mathcal{E}$ be a class of environments, w a prior over $\mathcal{E}$, and Π_R the set of policies satisfying resource constraints R. The *intelligence* of policy π is:

$$I(\pi; \mathcal{E}, R, w) = \mathbb{E}_{e \sim w} \left[\frac{V^{\pi}_{M_e}(b_0)}{V^{*}_{M_e,R}(b_0)} \right]$$

where $V^{*}_{M_e,R} = \sup_{\pi' \in \Pi_R} V^{\pi'}_{M_e}$.

This measures the expected fraction of achievable performance attained across environments.

2.6 The Detect-and-Reach Problem

We study a canonical problem where both observation and action matter.

Definition 2.8 (Detect-and-Reach POMDP)**.** Fix domain $X = \{1, \ldots, N\}$ (or $X \subseteq \mathbb{R}^d$), and:

- Target location $\theta \in X$ drawn uniformly: $\theta \sim \text{Uniform}(X)$
- Agent trajectory $(x_0, x_1, \ldots, x_T)$ with $|x_{t+1} - x_t| \leq v$
- Detection: At time t, if $|x_t - \theta| \leq r$, the agent learns θ exactly
- Capture: Agent captures θ if for some t, $|x_t - \theta| \leq a$ *and* θ is known
- Reward: $R = 1$ if captured by time T, $R = 0$ otherwise

The success probability $I(\pi) = \mathbb{P}[\text{capture}]$ depends on how the agent's trajectory interacts with the unknown target location.

2.7 Detection Model Assumptions

We make the following assumptions about the detection process:

1. **Perfect detection:** If $|x_t - \theta| \leq r$, the agent receives the exact value of θ with certainty.
2. **No false positives:** The agent never receives spurious detection signals.
3. **No partial information:** Outside the sensing radius r, the agent receives no information about θ.
4. **Instantaneous detection:** Detection occurs immediately upon entering sensing range.

These assumptions define a clean baseline model. Extensions to noisy detection, partial observability, or delayed information are natural directions for future work.

2.8 Scope of the Task

The detect-and-reach problem we analyze has the following characteristics:

- **Single target:** One hidden target θ.
- **Static target:** θ does not move.
- **Single episode:** One attempt to capture within horizon T.
- **Single agent:** No coordination with other agents.

- **No obstacles:** Free movement within the domain.
- **Deterministic dynamics:** Agent moves exactly as commanded.

The agent's uncertainty collapses completely at the moment of detection, transitioning from a uniform prior over X to perfect knowledge of θ.

3 The One-Dimensional Theory

3.1 Setup and Definitions

Consider the detect-and-reach problem on the discrete line $X = \{1, 2, \ldots, N\}$.

Definition 3.1 (Capturable Set)**.** The *capturable set* for a policy π is:

$$C(\pi) = \{\theta \in X : \theta \text{ is detected and subsequently captured under } \pi\}$$

For a fixed trajectory $\mathbf{x} = (x_0, \ldots, x_T)$, we write $C(\mathbf{x})$.

Definition 3.2 (Capacity)**.** The *capacity* is the maximum capturable set size:

$$C(v, T, r, a) = \max_{\pi} |C(\pi)|$$

Under a uniform prior, $I(\pi) = |C(\pi)|/N$, so maximizing $|C(\pi)|$ maximizes success probability.

Lemma 3.3 (Capture Feasibility)**.** *If detection occurs at time t_d with $|x_{t_d} - \theta| \le r$, then capture is feasible if and only if:*

$$|x_{t_d} - \theta| \le v(T - t_d) + a$$

Proof. After detection at time t_d, the agent can reach any position y with $|y - x_{t_d}| \le v(T - t_d)$. Capture requires $|y - \theta| \le a$ for some such y. By the triangle inequality, this is possible iff $|x_{t_d} - \theta| \le v(T - t_d) + a$. □

Definition 3.4 (Effective Radius)**.** The *effective radius* at time t is:

$$R_{\text{eff}}(t) = \min(r, v(T - t) + a)$$

This is the maximum distance at which a target can be both detected and subsequently captured.

3.2 Policy-to-Trajectory Reduction

The following lemma justifies why, in Cases A and B, we can analyze trajectories rather than general policies.

Lemma 3.5 (Search Path Reduction)**.** *For any policy π in Cases A or B, there exists a deterministic trajectory $\mathbf{x}^{\text{search}} = (x_0, x_1, \ldots, x_T)$ such that:*

1. *$\mathbf{x}^{\text{search}}$ has length at most vT;*
2. *Every target detected under π is detected along $\mathbf{x}^{\text{search}}$;*
3. *$C(\pi) \subseteq \bigcup_{t=0}^{T} \{\theta : |\theta - x_t^{\text{search}}| \le R_{\text{eff}}(t)\}$.*

Consequently, upper bounds on $|C(\mathbf{x})|$ over trajectories imply upper bounds on $|C(\pi)|$ over policies.

Proof. Before any detection occurs, all targets $\theta \in X$ produce identical observations (namely, "no detection"). Therefore, the policy π induces the same action sequence regardless of θ, generating a single deterministic *search path* $\mathbf{x}^{\text{search}}$.

A target θ is detected if and only if $|\theta - x_t^{\text{search}}| \leq r$ for some t. After detection, the policy may branch depending on the observed θ, but this branching affects only *which* detected targets are subsequently captured, not *which* targets are ever detected.

Proof of item (3): Let $\theta \in C(\pi)$ and let t_d be its detection time along $\mathbf{x}^{\text{search}}$. Then:

- $|\theta - x_{t_d}^{\text{search}}| \leq r$ (detection condition), and
- $|\theta - x_{t_d}^{\text{search}}| \leq v(T - t_d) + a$ (capture feasibility, by Lemma 3.3).

Hence $|\theta - x_{t_d}^{\text{search}}| \leq R_{\text{eff}}(t_d) = \min(r, v(T - t_d) + a)$, so $\theta \in \bigcup_{t=0}^{T} \{\theta : |\theta - x_t^{\text{search}}| \leq R_{\text{eff}}(t)\}$.

In Cases A and B, the capturable set is exactly this union:

- In Case A ($a \geq r$), any detected target can be captured from the detection position, so $C(\pi) = D(\mathbf{x}^{\text{search}})$.
- In Case B, a detected target at distance $d \leq r$ is capturable iff $d \leq v(T - t_d) + a$. The sweep strategy captures all such targets without needing to branch.

Thus, analyzing trajectories suffices to bound $|C(\pi)|$ in Cases A and B. □

Remark 3.6. This reduction fails in Case C, where all capturable targets are detected at $t = 0$ and the optimal policy must branch based on the detected location θ. In Case C, the search path is trivial (the agent need not move to detect), but post-detection pursuit is essential.

3.3 The Three Regimes

The relationship between r, a, v, and T determines qualitatively different behavior.

Definition 3.7 (Parameter Regimes)**.** (A) **Detection-limited** ($a \geq r$): Any detected target can be captured. Sensing is the bottleneck.

(B) **Coupled** ($a < r \leq vT + a$): Both detection and reach constrain capacity. The constraints interact nontrivially.

(C) **Reach-limited** ($r > vT + a$): Sensing exceeds useful range. The agent can detect more than it can possibly reach.

3.4 Main Theorem: 1D Capacity Bound

Theorem 3.8 (1D Detect-and-Reach Capacity)**.** *For any policy π in the 1D detect-and-reach POMDP:*

$$I(\pi) \leq \frac{C(v, T, r, a)}{N}$$

where the capacity C is:

$$C(v, T, r, a) = \begin{cases} \min(N, vT + 2r + 1) & a \geq r \quad \text{(Detection-limited)} \\ \min(N, vT + r + a + 1) & a < r \leq vT + a \quad \text{(Coupled)} \\ \min(N, 2(vT + a) + 1) & r > vT + a \quad \text{(Reach-limited)} \end{cases}$$

These bounds are achieved by:

- ***Cases A and B:*** *Monotonic sweep (non-adaptive trajectory)*

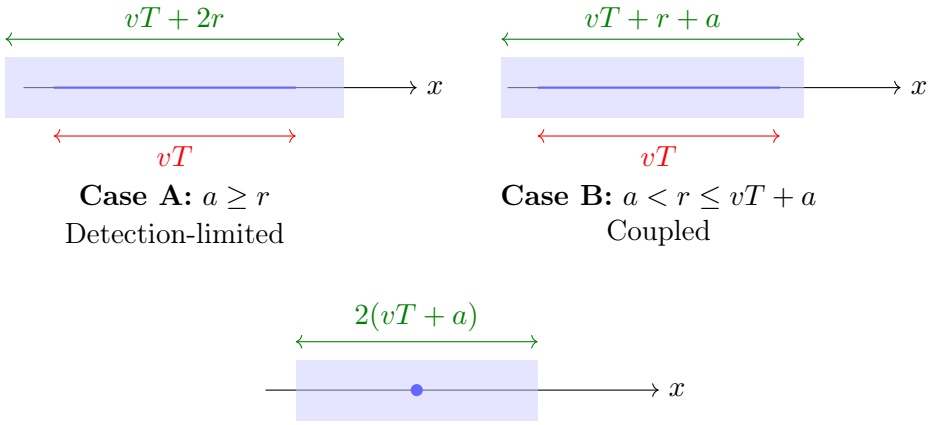

Case A: $a \geq r$
Detection-limited

Case B: $a < r \leq vT + a$
Coupled

Case C: $r > vT + a$
Reach-limited (detect-then-pursue)

Figure 1: The three regimes of the detect-and-reach problem. In Cases A and B, the optimal strategy is a monotonic sweep. In Case C, the optimal strategy is detect-then-pursue: detect at $t = 0$, then move toward the target.

- ***Case C:*** *Detect-then-pursue policy (observation-dependent)*

Remark 3.9 (Policy vs. Trajectory)**.** In Cases A and B, the optimal policy is a fixed trajectory that does not depend on observations—the agent commits to a sweep and captures whatever it encounters. In Case C, the optimal policy must branch based on the detected target location.

3.5 Proof of Theorem 3.8

We prove each case separately.

3.5.1 Case A: Detection-Limited ($a \geq r$)

When $a \geq r$, we have $R_{\text{eff}}(t) = r$ for all t (since $v(T - t) + a \geq a \geq r$). Any detected target can be captured immediately.

The capturable set equals the detection set:

$$C(\mathbf{x}) = D(\mathbf{x}) = \bigcup_{t=0}^{T} \{\theta : |x_t - \theta| \leq r\}$$

Lemma 3.10. *For any trajectory of length $\leq vT$, the detection set has diameter at most $vT + 2r$.*

Proof. The trajectory spans at most vT in space. The detection set is the trajectory thickened by r on each side, giving diameter at most $vT + 2r$. □

The rightward sweep $x_t = x_0 + vt$ achieves:

$$D_{\text{sweep}} = [x_0 - r, x_0 + vT + r] \cap X$$

with $|D_{\text{sweep}}| = \min(N, vT + 2r + 1)$. □

3.5.2 Case C: Reach-Limited ($r > vT + a$)

When $r > vT + a$, the sensing range exceeds the maximum reachable distance. This has a crucial consequence:

Lemma 3.11 (Immediate Detection in Case C)**.** *In Case C, any target θ with $|\theta - x_0| \leq vT + a$ is detected at $t = 0$.*

Proof. Since $r > vT + a$, the initial sensing ball $B(x_0, r)$ contains the entire reachability set $B(x_0, vT + a)$. Therefore, any target within reach is detected immediately. □

Lemma 3.12 (Capturable Set Bound in Case C)**.** *In Case C, $C(\pi) \subseteq [x_0 - vT - a, x_0 + vT + a]$ for any policy π.*

Proof. For capture at time t_c, we need $|x_{t_c} - \theta| \leq a$. By the triangle inequality:

$$|x_0 - \theta| \leq |x_0 - x_{t_c}| + |x_{t_c} - \theta| \leq v \cdot t_c + a \leq vT + a$$

□

Proposition 3.13 (Optimal Policy for Case C)**.** *In Case C, the optimal policy is* detect-then-pursue*: detect θ at $t = 0$, then move directly toward θ at speed v.*

Proof. By Lemma 3.11, any capturable target is detected at $t = 0$. After detection, the agent knows θ exactly. The agent can capture θ if and only if $|\theta - x_0| \leq vT + a$, which requires moving toward θ.

For any θ with $|\theta - x_0| \leq vT + a$:

- Detection occurs at $t = 0$ (since $r > vT + a \geq |\theta - x_0|$).
- The agent moves toward θ at speed v.
- At time $t_c = \max(0, (|\theta - x_0| - a)/v)$, the agent reaches within capture range.
- Since $|\theta - x_0| \leq vT + a$, we have $t_c \leq T$. Capture succeeds.

The capturable set is exactly $\{\theta : |\theta - x_0| \leq vT + a\}$, with size $2(vT + a) + 1$. □

Remark 3.14. A stationary strategy ($x_t = x_0$ for all t) would achieve only $|C| = 2a + 1$, far below the capacity. Movement is essential—it just occurs *after* and *in response to* detection, not as a pre-committed sweep.

3.5.3 Case B: Coupled ($a < r \leq vT + a$)

This is the most interesting case, where both constraints interact.

Lemma 3.15 (The Turnaround Penalty)**.** *In Case B, any non-monotonic trajectory achieves strictly less coverage than a monotonic sweep.*

Proof. Consider a trajectory that reverses direction at some time. Let t_1 be the time spent moving left before turning right. The leftmost position is $x_0 - vt_1$ at time t_1, and the rightmost position is $x_0 + vT - 2vt_1$ at time T.

Sub-case (i): $t_1 < t^* := T - (r - a)/v$

The effective radius at t_1 is r, so the span is:

$$R - L = (x_0 + vT - 2vt_1 + a) - (x_0 - vt_1 - r) = vT - vt_1 + r + a$$

This is maximized at $t_1 = 0$: $R - L = vT + r + a$.

Sub-case (ii): $t_1 \geq t^*$
The effective radius at t_1 is $v(T - t_1) + a < r$, giving span:

$$R - L = 2vT - 2vt_1 + 2a \leq 2r \leq vT + r + a$$

(using the Case B condition $r \leq vT + a$).
In both cases, the monotonic sweep ($t_1 = 0$) achieves the maximum. □

Lemma 3.16 (Capturable Set for Rightward Sweep)**.** *The rightward sweep in Case B captures exactly:*

$$C_{sweep} = [x_0 - r, x_0 + vT + a] \cap X$$

Proof. Targets in $[x_0 - r, x_0 + r]$*:* Detected at $t = 0$. Since $r \leq vT + a$ (Case B condition), capture is feasible.
Targets in $(x_0 + r, x_0 + vT + a]$*:* First detected at time $t_d = (\theta - r - x_0)/v$. The capture feasibility condition $r \leq v(T - t_d) + a$ reduces to $\theta \leq x_0 + vT + a$. ✓
Targets in $[x_0 - r, x_0)$*:* Detected at $t = 0$, captured since $a < r$ and $r \leq vT + a$ imply $|x_0 - \theta| \leq r \leq vT + a$. □

Combining Lemmas 3.15 and 3.16:

$$|C(\pi)| \leq vT + r + a + 1$$

with equality for the monotonic sweep. □

3.6 Continuity at Regime Boundaries

Proposition 3.17. *The capacity function $C(v, T, r, a)$ is continuous across regime boundaries.*

Proof. At $r = a$ (A↔B boundary):

- Case A: $vT + 2a + 1$
- Case B: $vT + a + a + 1 = vT + 2a + 1$ ✓

At $r = vT + a$ (B↔C boundary):

- Case B: $vT + (vT + a) + a + 1 = 2vT + 2a + 1$
- Case C: $2(vT + a) + 1 = 2vT + 2a + 1$ ✓

□

4 The Two-Dimensional Theory

4.1 Setup

We extend to the plane $X \subseteq \mathbb{R}^2$. As noted in Section 2.2, we work with continuous time $t \in [0, T]$ for the 2D analysis. The agent follows a continuous trajectory $\gamma : [0, T] \to \mathbb{R}^2$ with $\|\dot{\gamma}(t)\| \leq v$.

Definition 4.1 (2D Capturable Set)**.** For trajectory γ with sensing range r and capture range a:

$$C(\gamma) = \bigcup_{t=0}^{T} B(\gamma(t), R_{\text{eff}}(t))$$

where $B(c, \rho)$ is the closed disk of radius ρ centered at c.

Remark 4.2 (Policy-to-Trajectory Reduction in 2D)**.** As in Lemma 3.5 for the 1D case, before any detection event all targets induce identical observations ("no detection") and hence the policy generates the same open-loop search trajectory γ. For the purpose of upper bounding $\mu(C(\pi))$, it suffices to bound $\mu(C(\gamma))$ over all admissible search trajectories γ of arc length $\leq vT$. Post-detection branching affects which detected targets are actually pursued, but cannot expand the union $\bigcup_t B(\gamma(t), R_{\text{eff}}(t))$ that defines the capturable region. Thus Theorem 4.4 bounds capacity over *policies*, not merely over trajectories.

4.2 The Stadium Geometry

Definition 4.3 (Stadium)**.** The *stadium* (or *discorectangle*) $\mathcal{S}(L, \rho)$ is the Minkowski sum of a line segment of length L with a disk of radius ρ:

$$\mathcal{S}(L, \rho) = \{x \in \mathbb{R}^2 : d(x, \text{segment}) \leq \rho\}$$

Its area is $\text{Area}(\mathcal{S}(L, \rho)) = 2\rho L + \pi\rho^2$.

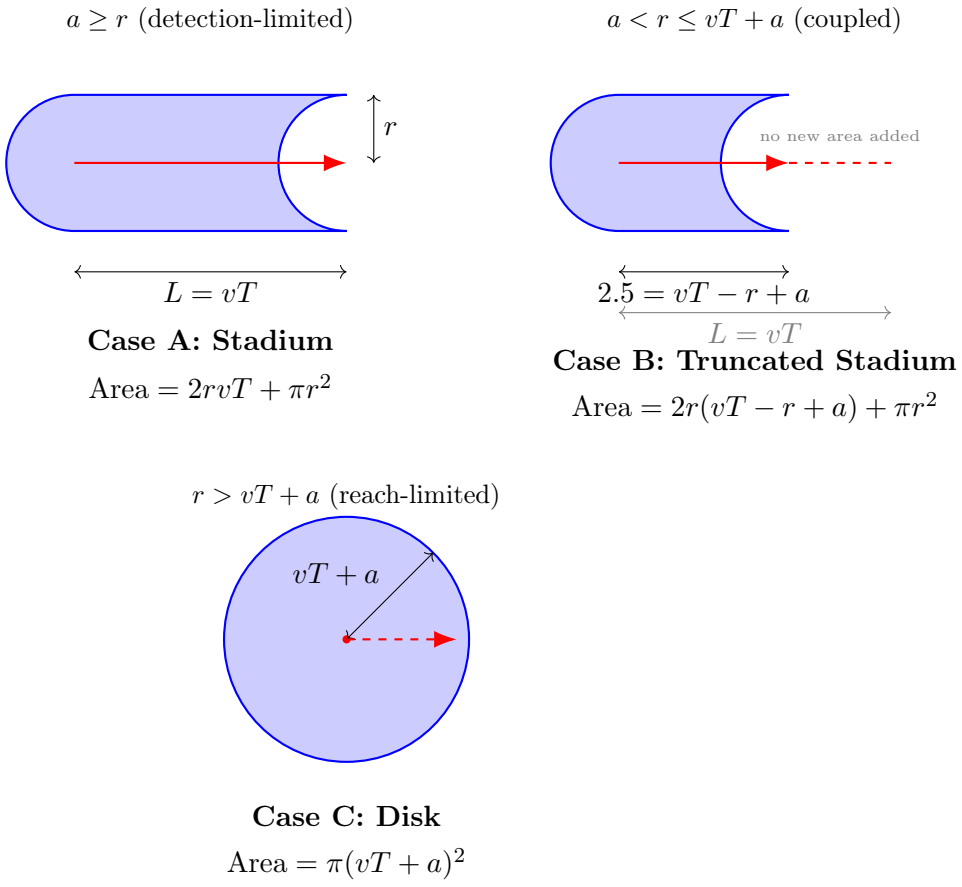

Figure 2: Geometric shapes of the 2D capturable region in the three regimes. In Case A, the agent sweeps a straight path of length vT, producing a full stadium of radius r. In Case B, only the first $L_{\text{eff}} = vT - r + a$ units of the path add area, yielding a truncated stadium; the remaining motion occurs inside the already-covered tube. In Case C, sensing is so large that all capturable points are detected at $t = 0$, and the capturable region is a disk of radius $vT + a$ centered at the initial position.

4.3 Main Theorem: 2D Capacity Bound

Theorem 4.4 (2D Detect-and-Reach Capacity)**.** *For any policy π in the 2D detect-and-reach POMDP:*

$$\mu(C(\pi)) \leq \mathcal{C}_{2D}(v, T, r, a)$$

where:

$$\mathcal{C}_{2D} = \begin{cases} 2rvT + \pi r^2 & a \geq r \quad \text{(Stadium)} \\ 2r(vT - r + a) + \pi r^2 & a < r \leq vT + a \quad \text{(Truncated Stadium)} \\ \pi(vT + a)^2 & r > vT + a \quad \text{(Disk)} \end{cases}$$

These bounds are achieved by:

- ***Cases A and B:*** *Straight-line sweep*
- ***Case C:*** *Detect-then-pursue policy*

4.4 Proof of Theorem 4.4

4.4.1 Case C: The Disk (Reach-Limited)

Lemma 4.5. *In Case C ($r > vT + a$), $C(\gamma) \subseteq B(\gamma(0), vT + a)$ for any trajectory.*

Proof. The 1D argument extends directly. For any capturable point θ at time t:

$$\|\gamma(0) - \theta\| \leq \|\gamma(0) - \gamma(t)\| + \|\gamma(t) - \theta\| \leq vt + R_{\text{eff}}(t) = vt + v(T - t) + a = vT + a$$

□

The detect-then-pursue policy (detect at $t = 0$, move toward θ) achieves exactly the disk $B(\gamma(0), vT + a)$.

4.4.2 Case A: The Stadium (Detection-Limited)

When $a \geq r$, we have $R_{\text{eff}}(t) = r$ for all t.

Lemma 4.6 (Straight-Line Optimality via Steiner Formula)**.** *Among all rectifiable curves γ of length L, the straight line uniquely maximizes* $\text{Area}(\gamma \oplus B_r)$.

Proof. We restrict attention to simple (non-self-intersecting) C^1 curves; the general case follows by approximation.

For any such curve γ of length L, the Steiner-type tube formula gives:

$$\text{Area}(\gamma \oplus B_r) = 2rL + \pi r^2 - \text{Overlap}(\gamma, r)$$

where $\text{Overlap}(\gamma, r) \geq 0$ is the area of the r-tube counted with multiplicity greater than one (see Appendix C).

Claim: $\text{Overlap}(\gamma, r) = 0$ if and only if γ is a straight line segment.

Proof of claim: Consider the normal map $\Phi(s, u) = \gamma(s) + u\mathbf{n}(s)$ for arc-length parameter $s \in [0, L]$ and transverse coordinate $u \in [-r, r]$.

The Jacobian determinant is $\det J_\Phi(s, u) = 1 - \kappa(s)u$, where $\kappa(s)$ is the signed curvature.

Straight line case: If γ is a straight line, then $\kappa(s) \equiv 0$, so $\det J_\Phi = 1 > 0$ everywhere. The normal lines are parallel and do not intersect, so Φ is injective on the interior of $[0, L] \times (-r, r)$. Hence Overlap $= 0$.

Curved case: If $\kappa(s_0) \neq 0$ at some point s_0, then the osculating circle at s_0 has radius $\rho_0 = 1/|\kappa(s_0)|$. The center of this circle lies at distance ρ_0 along the normal. Two cases arise:

- If $\rho_0 < r$ (tight curvature), the normal map has $\det J_\Phi < 0$ for $|u| > \rho_0$, indicating fold-over within the tube. The offset boundary self-intersects locally.
- If $\rho_0 \geq r$ everywhere (gentle curvature), local injectivity holds, but normal lines at different points $s_1 \neq s_2$ may still intersect within the tube if the curve bends cumulatively. For any non-straight curve of positive length, there exist s_1, s_2 whose normal lines meet at distance $< r$ from at least one of them.

In either case, Φ fails to be globally injective, so Overlap > 0. Formally, this is a direct consequence of Theorem C.2 in Appendix C: any nonzero curvature or global bending of a simple curve induces self-overlap in the r-tube, so $\text{Overlap}(\gamma, r) > 0$ unless γ is a straight segment.

This establishes that the maximum area $2rL + \pi r^2$ is achieved uniquely by straight lines. □

With $L = vT$, the maximum area is $2rvT + \pi r^2$, achieved by a straight-line trajectory.

4.4.3 Case B: The Truncated Stadium (Coupled)

In Case B, the effective radius transitions from r to shrinking at time $t^* = T - (r - a)/v$.

Lemma 4.7 (Internal Tangency)**.** *For $t > t^*$ on a straight-line trajectory, $B(\gamma(t), R_{\text{eff}}(t)) \subset B(\gamma(t^*), r)$.*

Proof. For a straight-line trajectory moving at speed v:

- Position at time t: $\gamma(t) = \gamma(t^*) + v(t - t^*) \cdot \mathbf{e}$
- Radius at time t: $R_{\text{eff}}(t) = r - v(t - t^*)$

The "front" of $B(\gamma(t), R_{\text{eff}}(t))$ (in direction $\mathbf{e}$):

$$\gamma(t) + R_{\text{eff}}(t) \cdot \mathbf{e} = \gamma(t^*) + v(t - t^*)\mathbf{e} + (r - v(t - t^*))\mathbf{e} = \gamma(t^*) + r\mathbf{e}$$

This equals the front of $B(\gamma(t^*), r)$—the disks are internally tangent at the front.
The "back" of $B(\gamma(t), R_{\text{eff}}(t))$:

$$\gamma(t) - R_{\text{eff}}(t) \cdot \mathbf{e} = \gamma(t^*) + (2v(t - t^*) - r)\mathbf{e}$$

Since $t > t^*$, this is strictly to the right of $\gamma(t^*) - r\mathbf{e}$.
Thus $B(\gamma(t), R_{\text{eff}}(t)) \subset B(\gamma(t^*), r)$ for all $t > t^*$. □

Consequence: Phase 2 ($t > t^*$) adds zero new area. The capturable region is exactly the stadium swept during Phase 1:

$$C(\gamma) = \mathcal{S}(L_{\text{eff}}, r) \quad \text{where} \quad L_{\text{eff}} = vt^* = vT - (r - a)$$

Area: $\text{Area} = 2r \cdot L_{\text{eff}} + \pi r^2 = 2r(vT - r + a) + \pi r^2$.

4.5 Continuity Verification

At $r = a$:

$$\mathcal{C}_{2D}^{(B)} = 2a(vT - a + a) + \pi a^2 = 2avT + \pi a^2 = \mathcal{C}_{2D}^{(A)} \quad \checkmark$$

At $r = vT + a$:

$$\mathcal{C}_{2D}^{(B)} = 2(vT + a)(0) + \pi(vT + a)^2 = \pi(vT + a)^2 = \mathcal{C}_{2D}^{(C)} \quad \checkmark$$

5 Empirical Validation

5.1 1D Monte Carlo Stress Test

We validated the 1D theorem by simulating 5,000 random trajectories in the coupled regime (Case B) with parameters $v = 1$, $T = 20$, $a = 5$, $r = 15$.

Results:

- Theoretical bound: $C = vT + r + a + 1 = 41$
- Sweep strategy achieves: 41 (exactly)
- Maximum over random trajectories: 39

The gap of 2 between random maximum and the bound confirms the turnaround penalty: any deviation from monotonic motion loses coverage.

5.2 2D Grid Simulation

We tested the 2D bounds on a discrete grid, comparing straight sweeps, spirals, and random walks across all three regimes.

Results:

- Straight sweeps track the theoretical bound across all regimes
- Spirals underperform due to curvature penalty (self-overlapping coverage)
- The sweep-spiral gap is largest in Case B, where the interaction between sensing and reach is most significant

5.3 Discretization Effects

Simulated areas slightly exceeded theoretical predictions due to the Gauss circle problem: grid approximations of disks include boundary pixels, adding $O(\sqrt{\text{Area}})$ error.

Specifically, for a shape with area A and perimeter P, the grid approximation error is $O(P) = O(\sqrt{A})$. Thus the relative error vanishes as the scale increases:

$$\frac{\text{Error}}{\text{Area}} = O\left(\frac{\sqrt{A}}{A}\right) = O(A^{-1/2}) \to 0$$

This confirms the continuous bounds are correct in the limit.

6 Composition of Cognitive Light Cones on a Line

We now study the simplest compositional setting: multiple identical agents on a 1D line with full communication, in the detection-limited regime $a \geq r$ (Case A in Definition 3.7). The goal is to characterize how detect-and-reach *capacity* scales with the number of agents k.

6.1 Multi-Agent Model on a Finite Interval

We work on a finite 1D domain $X = \{1, 2, \ldots, N\}$.

Definition 6.1 (Multi-Agent Detect-and-Reach Model)**.** Fix parameters $v \in \mathbb{N}$, $T \in \mathbb{N}$, sensing radius $r \in \mathbb{N}$, and capture radius $a \in \mathbb{N}$ with $a \geq r$ (detection-limited regime). Let:

- $k \in \mathbb{N}$ be the number of agents.

- $\theta \in X$ be the (static) target location, drawn uniformly from X.
- $x_t^i \in X$ be the position of agent $i \in \{1, \dots, k\}$ at time $t \in \{0, \dots, T\}$, with speed constraint

$$|x_{t+1}^i - x_t^i| \le v \quad \text{for all } i, t.$$

- *Detection*: at time t, agent i detects the target if $|x_t^i - \theta| \le r$.
- *Capture*: the target is captured if for some (i, t) we have $|x_t^i - \theta| \le a$ and θ is known.

We assume the same perfect detection model as in Section 2.7: whenever $|x_t^i - \theta| \le r$, agent i learns the exact value of θ, with no false positives or negatives. Under **full communication (FC)**, all detection events (time, agent index, and detected location) are broadcast instantly and are common knowledge among all agents.

Definition 6.2 (Joint Policies and Success)**.** A *joint policy* is a tuple $\pi = (\pi^1, \dots, \pi^k)$ where each π^i maps the common information history (observations and actions of all agents) to the next action of agent i.

For a joint policy π, we define the multi-agent capturable set as

$$C_k(\pi) = \big\{\theta \in X : \theta \text{ is detected by some agent and subsequently captured by time } T \text{ under } \pi\big\}.$$

Definition 6.3 (Multi-Agent Capacity)**.** The k-agent capacity in the detection-limited regime is

$$C_k(v, T, r, a) = \max_{\pi} |C_k(\pi)|.$$

Under the uniform prior on θ, the optimal success probability is $C_k(v, T, r, a)/N$.

For $k = 1$, this recovers the single-agent capacity $C_1(v, T, r, a) = C(v, T, r, a)$ of Theorem 3.8 in the case $a \ge r$.

6.2 Search-Path Reduction for Teams

In the single-agent case (Lemma 3.5), we showed that before detection the agent follows a deterministic search path. The same structure holds for multiple agents under full communication.

Lemma 6.4 (Multi-Agent Search-Path Reduction (FC, 1D))**.** *Consider the k-agent model of Definition 6.1 with full communication and $a \ge r$. For any joint policy π, there exists a joint* search trajectory

$$\mathbf{x}^{\text{search}} = \big((x_0^1, \dots, x_0^k), \dots, (x_T^1, \dots, x_T^k)\big),$$

such that:

1. *For each i, the path $(x_0^i, \dots, x_T^i)$ is deterministic and satisfies $|x_{t+1}^i - x_t^i| \le v$.*
2. *Any target that is ever detected under π is detected along the joint search trajectory $\mathbf{x}^{\text{search}}$.*
3. *The capturable set of π is contained in the union of r-thickenings around the search paths:*

$$C_k(\pi) \subseteq \bigcup_{i=1}^{k} \bigcup_{t=0}^{T} \{\theta \in X : |x_t^i - \theta| \le r\}.$$

In particular, upper bounds on the size of this union over all admissible joint search trajectories yield upper bounds on $C_k(v, T, r, a)$.

Proof sketch. Before any detection event, all targets $\theta \in X$ produce identical common observations: the joint observation history is "no detections" for all agents. Hence, as in Lemma 3.5, the joint policy π induces a deterministic open-loop sequence of joint actions, and thus a deterministic joint search trajectory $\mathbf{x}^{\text{search}}$.

Any target that is eventually detected must first be detected at some time t along this pre-detection phase. By the detection model and full communication, once some agent detects the target, all agents know θ exactly. Because $a \geq r$ and capture requires knowledge, any detected target can be captured immediately from the detecting agent's position, so in this regime the capturable set coincides with the detection set. This yields the containment in item (3). A full formalization mirrors the single-agent argument and is omitted. □

Thus, in the detection-limited FC setting, we can reason entirely about geometric unions of 1D "tubes"

$$\bigcup_{i=1}^{k} \bigcup_{t=0}^{T} [x_t^i - r,\, x_t^i + r]$$

generated by k deterministic search paths of total length at most vT each.

6.3 A First Composition Theorem on a Line

We now state a first capacity result showing that in the detection-limited regime, multi-agent capacity scales linearly with the number of agents k until it saturates at the domain size N.

For clarity, we first ignore boundary effects and work in a regime where the agents can be placed far from the endpoints of X.

Definition 6.5 (Bulk Regime)**.** We say that (N, k, v, T, r, a) is in the *bulk regime* if

$$N \geq 2k(vT + 2r + 1),$$

so that agents and their capturable sets can be arranged with disjoint interiors away from the boundaries of X.

Theorem 6.6 (Multi-Agent Capacity on a Line, Detection-Limited, FC)**.** *Fix $v, T, r, a \in \mathbb{N}$ with $a \geq r$ and consider the k-agent model on $X = \{1, \ldots, N\}$ with full communication. Then:*

1. *(**Upper bound, all** N) For any N,*

$$C_k(v, T, r, a) \leq \min\big\{\, N,\ k\,(vT + 2r + 1)\,\big\}.$$

2. *(**Achievability up to edge terms**) In the bulk regime,*

$$C_k(v, T, r, a) \geq k\,(vT + 2r + 1) - O(k),$$

where the $O(k)$ term accounts for discrete placement and small overlaps at the boundaries of the capturable intervals.

In particular, for fixed (v, T, r, a) and k with $N \to \infty$,

$$C_k(v, T, r, a) = k\,(vT + 2r + 1) - O(k),$$

so the capacity scales linearly in k. Equivalently, in the bulk regime the team capturable set is, up to constant-order boundary corrections,

$$C_k(v, T, r, a) \approx \bigsqcup_{i=1}^{k} C_1^{(i)},$$

a disjoint union of k single-agent capturable sets, each of size $vT + 2r + 1$.

Proof sketch. **Upper bound.** By Lemma 6.4, the capturable set is contained in the union

$$U = \bigcup_{i=1}^{k} \bigcup_{t=0}^{T} [x_t^i - r,\, x_t^i + r] \cap X$$

for some admissible joint search trajectory. For each agent i, the single-agent 1D argument in the detection-limited case (Section 3) shows that

$$\left| \bigcup_{t=0}^{T} [x_t^i - r,\, x_t^i + r] \cap X \right| \leq vT + 2r + 1.$$

Therefore

$$|U| \leq \sum_{i=1}^{k} \left| \bigcup_{t=0}^{T} [x_t^i - r,\, x_t^i + r] \cap X \right| \leq k(vT + 2r + 1),$$

and $|U| \leq N$ trivially, giving the stated upper bound.

Lower bound (bulk regime). In the bulk regime, we can place the k agents at time $t = 0$ so that their initial positions are separated by at least $(vT + 2r + 1)$ and lie away from the endpoints of X. For each agent i, assign a disjoint interval $I_i \subset X$ of length exactly $vT + 2r + 1$, and let agent i follow the single-agent optimal sweep policy on I_i from Theorem 3.8 (Case A). By construction, each agent i captures all targets $\theta \in I_i$, and the I_i are disjoint.

Thus there exists a joint policy π with

$$|C_k(\pi)| \geq \sum_{i=1}^{k} |I_i| = k(vT + 2r + 1).$$

On the discrete lattice X, interval endpoints must be integers, so in general we can lose at most a constant number of points per interval due to rounding and spacing constraints, yielding the $O(k)$ correction term. A detailed combinatorial placement argument can make the constant explicit. □

Remark 6.7 (First Composition Law)**.** Theorem 6.6 gives a first quantitative composition result for cognitive light cones on a line in the simplest regime:

$$\text{Team capacity} \;\approx\; \sum_{i=1}^{k} (\text{single-agent capacity})$$

until saturation at the domain size N. In the detection-limited FC setting, the collective light cone of k agents is, to first order, just the union of k independent single-agent light cones.

7 Example: Corridor Coverage Design

To demonstrate the practical utility of the theory, we apply the results to a concrete engineering scenario: designing a multi-robot system for hospital corridor sanitation. This example illustrates how the abstract "capacity" formulas can be inverted to derive hardware procurement requirements.

7.1 Scenario Definition

Consider a hospital hallway of length $N = 100$ meters. A team of k cleaning robots must be able to detect and sanitize a random spill anywhere in the corridor within a time limit of $T = 60$ seconds.

The robots have the following specifications:

- **Speed (v):** The maximum speed of the robot base.
- **Sensor Range (r):** The radius of the onboard Lidar/camera system.
- **Actuation Range (a):** The reach of the cleaning arm, fixed at $a = 0.5$ meters.

The design question is: *Given the coverage goal, how many robots do we need, and what specifications (v, r) must they have?*

7.2 Inverting the Capacity Theorem

We assume the system operates in the **Coupled Regime** (Case B), which is typical for robotics where $a < r \ll vT$. From Theorem 3.8, the capacity of a single robot is:

$$C_{\text{robot}} \approx vT + r + a$$

To guarantee 100% coverage of the domain N, the required number of robots k is:

$$k \geq \left\lceil \frac{N}{C_{\text{robot}}} \right\rceil = \left\lceil \frac{100}{v(60) + r + 0.5} \right\rceil$$

This equation defines the trade-off surface between hardware cost (speed, sensor quality) and fleet size.

7.3 The Procurement Chart

We visualize this trade-off in Figure 3, which acts as a "flight envelope" for the cleaning system.

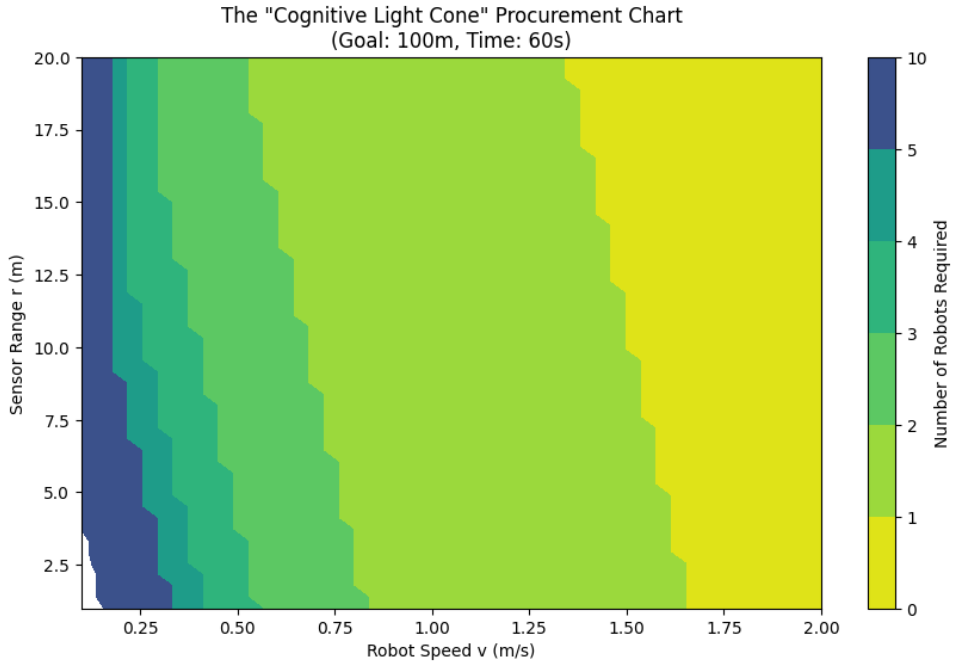

Figure 3: The "Procurement Chart" for the corridor coverage problem ($N = 100$m, $T = 60$s). The color indicates the minimum number of robots (k) required for full coverage. Vertical bands indicate that capacity is dominated by speed (v) rather than sensing range (r).

Analysis of the Chart:

1. **Speed Dominance:** The contour bands are nearly vertical. Because $T = 60$, every 1 m/s increase in speed adds 60 meters to the light cone, whereas every 1 meter increase in sensor range adds only 1 meter.

2. **The "Blue Trench":** For $v < 0.25$ m/s, the robots are too slow to cover the area even with infinite sensor range (reaching the Case C limit). Fleet size requirements explode ($k > 10$).

3. **The "Yellow Zone":** For $v > 1.6$ m/s, a single robot ($k = 1$) suffices regardless of sensor range.

Design Recommendation: For this specific scenario, budget should be prioritized for motor speed rather than long-range sensors, as the system is heavily reach-constrained rather than detection-constrained.

8 Discussion

8.1 Physical Interpretation of the Regimes

The three regimes have intuitive interpretations:

Case A (Detection-Limited): The agent can always catch what it sees. The challenge is purely exploratory—sweep as much territory as possible. Optimal strategy: monotonic sweep.

Case B (Coupled): There exists a critical time $t^* = T-(r-a)/v$ where the agent transitions from "sensor-limited" to "fuel-limited." Before t^*, aggressive exploration is optimal. After t^*, the detection wave's "front" freezes—the agent can still move, but the effective sensing radius shrinks to match remaining reach. Optimal strategy: monotonic sweep (the Phase 2 nesting means no benefit from observation-dependent behavior).

Case C (Reach-Limited): Sensing range exceeds useful range. All capturable targets are detected immediately at $t = 0$. The agent then knows exactly where to go. Optimal strategy: detect-then-pursue.

8.2 Biological Interpretation

Levin's cognitive light cone concept describes how biological agents—from cells to organisms—exhibit goal-directed behavior at multiple scales. Our formalization provides a quantitative interpretation:

- A "single agent" in our model corresponds to a minimal biological controller: a cell, a neural circuit, an immune response unit.
- The **capacity bound** represents the maximum spatial region that level of biological organization can meaningfully govern.
- **Nested biological intelligence** corresponds to nested light cones: cells compose into tissues, tissues into organs, organs into organisms. Each level has characteristic (r, a, v, T) parameters.
- **Cancer** (in Levin's framing) corresponds to coupling failure: when cells shrink their light cones from organism-level to cell-level goals.

The mathematics of composition—when collective light cones expand versus fragment—remains an important open problem connecting our framework to developmental biology.

8.3 Limitations

Our analysis makes several simplifying assumptions:

- **Static target:** θ does not move. Moving targets introduce pursuit-evasion dynamics.

- **Perfect detection:** No noise, no false positives/negatives. Real sensors have uncertainty.
- **Single target:** One hidden θ. Multiple targets require coverage optimization.
- **Single agent:** No coordination. Multi-agent settings require Dec-POMDP analysis.
- **No obstacles:** Free movement. Obstacles introduce path-planning constraints.
- **Deterministic dynamics:** Agent moves exactly as commanded. Stochastic motion adds uncertainty.
- **Unlimited memory/computation:** Agent can compute optimal pursuit. Bounded rationality is not modeled.
- **Unconstrained angular movement (2D):** Agent can change direction instantly. Turn-rate constraints would modify the geometry.

Each of these represents a natural extension direction.

9 Conclusion

We have developed a rigorous geometric theory of resource-bounded goal achievement. The main contributions are:

1. **Formalization:** The cognitive light cone as observability $\cup$ reachability in POMDP language, with explicit time/space conventions and detection model assumptions.
2. **1D Theorem:** Tight bounds on capturable set size with three distinct regimes, sharp transitions, and regime-specific optimal strategies (sweep for A/B, detect-then-pursue for C).
3. **2D Theorem:** Stadium geometry bounds with rigorous proof of straight-line optimality via Steiner-type curvature penalty argument.
4. **Design Application:** A concrete demonstration of how these bounds translate into engineering design rules for multi-robot systems.

These results provide the first explicit "goal size $\leq f$(resources)" inequalities for spatial POMDPs, bridging control theory, POMDP planning, and Levin's biology of diverse intelligence.

The framework opens several directions: multi-agent composition, stochastic dynamics, memory constraints, and ultimately a unified theory of how intelligence scales with resources across levels of biological and artificial organization.

Acknowledgments

This work benefited from extensive iterative development, including systematic translation to POMDP foundations, identification of proof gaps, rigorous verification of geometric arguments, and critical review that identified and corrected errors in the original Case C analysis.

References

El Yacoubi, S., et al. (2002). Regional controllability with cellular automata models. In *Cellular Automata*, pages 357–367. Springer.

Kaelbling, L. P., Littman, M. L., and Cassandra, A. R. (1998). Planning and acting in partially observable stochastic domains. *Artificial Intelligence*, 101(1-2):99–134.

Kara, A. D., Saldi, N., and Yüksel, S. (2021). Convergence of finite memory Q-learning for POMDPs and near optimality of learned policies. *arXiv preprint arXiv:2103.12158*.

Legg, S. and Hutter, M. (2007). Universal intelligence: A definition of machine intelligence. *Minds and Machines*, 17(4):391–444.

Levin, M. (2019). The computational boundary of a "self": Developmental bioelectricity drives multicellularity and scale-free cognition. *Frontiers in Psychology*, 10:2688.

Levin, M. (2025). Artificial intelligences: A bridge toward diverse intelligence and humanity's future. *Advanced Intelligent Systems*, (to appear).

Nair, G. N., Fagnani, F., Zampieri, S., and Evans, R. J. (2007). Feedback control under data rate constraints: An overview. *Proceedings of the IEEE*, 95(1):108–137.

Oliehoek, F. A. and Amato, C. (2016). *A Concise Introduction to Decentralized POMDPs*. Springer.

Wu, F., Zilberstein, S., and Chen, X. (2011). Online planning for multi-agent systems with bounded communication. *Artificial Intelligence*, 175(2):487–511.

A Summary of Notation

B Proof Details for the Turnaround Penalty

We provide the complete case analysis for Lemma 3.15.

Consider a trajectory that spends time t_1 moving left before reversing to move right. The leftmost position is $x_0 - vt_1$ at time t_1, and the rightmost position is $x_0 - vt_1 + v(T - t_1) = x_0 + vT - 2vt_1$ at time T.

Sub-case (i): $t_1 < t^*$

The effective radius at t_1 is r, so:

$$L = x_0 - vt_1 - r$$
$$R = x_0 + vT - 2vt_1 + a$$

Span: $R - L = vT - vt_1 + r + a$

This is maximized at $t_1 = 0$: $R - L = vT + r + a$.

Sub-case (ii): $t_1 \geq t^*$

The effective radius at t_1 is $v(T - t_1) + a$, so:

$$L = x_0 - vt_1 - v(T - t_1) - a = x_0 - vT - a$$
$$R = x_0 + vT - 2vt_1 + a$$

Span: $R - L = 2vT - 2vt_1 + 2a$

Since $t_1 \geq t^* = T - (r - a)/v$:

$$R - L \leq 2r \leq vT + r + a$$

(using the Case B condition $r \leq vT + a$).

Thus monotonic sweep ($t_1 = 0$) achieves the maximum span.

Symbol	Meaning
X	Spatial domain
θ	Target location (hidden)
$x_t, \gamma(t)$	Agent position at time t
v	Maximum speed (distance per unit time)
T	Time horizon (discrete steps)
r	Sensing range
a	Actuation (capture) range
$R_{\text{eff}}(t)$	Effective radius: $\min(r, v(T-t)+a)$
L_{eff}	Effective sweep length in Case B: $vT - r + a$
t^*	Transition time in Case B: $T - (r-a)/v$
$\mathbf{x}^{\text{search}}$	Pre-detection search trajectory (Cases A, B)
$C(\pi)$	Capturable set under policy π
$C(\mathbf{x})$	Capturable set under trajectory $\mathbf{x}$
$C(v, T, r, a)$	Capacity: $\max_\pi \lvert C(\pi)\rvert$
$\mathcal{O}(x, r)$	Observability set (sensing ball)
$\mathcal{R}(x, a, T)$	Reachability set
$L_t(T)$	Cognitive light cone at time t
$\mathcal{S}(L, \rho)$	Stadium: segment of length $L \oplus$ disk of radius ρ

Table 1: Summary of notation used throughout the paper.

C The Steiner Tube Formula

For completeness, we state the classical results that underlie the 2D optimality argument.

Theorem C.1 (Steiner Formula for Convex Bodies)**.** *Let $K \subset \mathbb{R}^2$ be a convex body with perimeter P and area A. The area of its r-neighborhood (Minkowski sum with a disk of radius r) is:*

$$\text{Area}(K \oplus B_r) = A + Pr + \pi r^2$$

For a line segment (perimeter $2L$, area 0), this gives Area $= 2Lr + \pi r^2$, which is the stadium formula.

Theorem C.2 (Tube Formula for Curves)**.** *Let $\gamma : [0, L] \to \mathbb{R}^2$ be a simple C^2 curve parameterized by arc length, with signed curvature $\kappa(s)$. Define the normal map $\Phi(s, u) = \gamma(s) + u\mathbf{n}(s)$ for $u \in [-r, r]$.*

If $|\kappa(s)| < 1/r$ for all s (i.e., the radius of curvature exceeds r everywhere), then Φ is a local diffeomorphism on $(0, L) \times (-r, r)$, and:

$$\text{Area}(\gamma \oplus B_r) = \int_0^L \int_{-r}^{r} |1 - \kappa(s)u| \, du \, ds + \pi r^2 - \textit{Overlap}$$

where the overlap term accounts for global (non-local) self-intersections of the tube.

If γ is a straight line ($\kappa \equiv 0$), then Φ is globally injective, overlap is zero, and the formula reduces to $2rL + \pi r^2$.

The key insight for our application is that any deviation from straightness—whether through local curvature or global bending—introduces overlap that strictly reduces the covered area below the maximum $2rL + \pi r^2$.

D Design Tool Source Code

We include the Python source code used to generate the procurement chart in Section 7. This script computes the required fleet size k across the parameter space (v, r) for the specified goal.

Listing 1: Python script for generating the procurement chart

```python
import numpy as np
import matplotlib.pyplot as plt

def calculate_capacity_1d(v, T, r, a):
    """
␣␣␣␣Returns␣the␣capacity␣(meters␣covered)␣for␣a␣single␣agent.
␣␣␣␣"""
    if a >= r: # Case A
        return v * T + 2 * r
    elif r > v * T + a: # Case C
        return 2 * (v * T + a)
    else: # Case B (Coupled)
        return v * T + r + a

# Simulation Parameters
N_goal = 100    # Goal: 100m corridor
T_fixed = 60    # Time: 60 seconds
a_fixed = 0.5   # Arm reach: 0.5m

# Create Grid for Contour Plot
v_range = np.linspace(0.1, 2.0, 50)  # Speed: 0.1 to 2.0 m/s
r_range = np.linspace(1, 20, 50)     # Sensor: 1 to 20 m
X, Y = np.meshgrid(v_range, r_range)
Z = np.zeros_like(X)

# Calculate Required Robots (k)
for i in range(len(r_range)):
    for j in range(len(v_range)):
        cap = calculate_capacity_1d(X[i,j], T_fixed, Y[i,j], a_fixed)
        robots_needed = np.ceil(N_goal / cap)
        Z[i,j] = robots_needed

# Plotting
plt.figure(figsize=(8, 6))
cp = plt.contourf(X, Y, Z, levels=[0, 1, 2, 3, 4, 5, 10], cmap='
    viridis_r')
cbar = plt.colorbar(cp)
cbar.set_label('Number␣of␣Robots␣Required')
plt.xlabel('Robot␣Speed␣v␣(m/s)')
plt.ylabel('Sensor␣Range␣r␣(m)')
plt.title(f'Procurement␣Chart␣(Goal:␣{N_goal}m,␣Time:␣{T_fixed}s)')
plt.tight_layout()
plt.show()
```